

Defect structure and charge transport in solid solutions  $\text{Ba}_{1-x}\text{La}_x\text{F}_{2+x}$ 

H. W. den Hartog, K. F. Pen, and J. Meuldijk

*Solid State Physics Laboratory, 1 Melkweg, 9718-EP Groningen, The Netherlands*

(Received 11 March 1983)

In this paper we have investigated the defect structure and the charge-transport properties of solid solutions of the type  $\text{Ba}_{1-x}\text{La}_x\text{F}_{2+x}$ . The defect structure has been studied by means of samples which had been doped slightly with trivalent gadolinium ions. These probes have been employed to investigate the surrounding crystal lattice, which contains in some cases large amounts of trigonal  $\text{La}^{3+}\text{-F}_i^-$  dipoles. It appears that the  $\text{Gd}^{3+}$  impurities do not participate in an eventual clustering process, because we have not observed EPR signals with significant intensities which can be assigned to clusters. In the solid solutions studied in this paper we have observed two different dipolar defects: (a) the nearest-neighbor (NN) or tetragonal  $\text{La}^{3+}\text{-F}_i^-$  dipole and (b) the next-nearest-neighbor (NNN) or trigonal  $\text{La}^{3+}\text{-F}_i^-$  dipole, the latter being the more dominant defect. The concentration ratio of the NN and NNN dipoles varies with the concentration of  $\text{La}^{3+}$  ions in the sample. With increasing  $\text{La}^{3+}$  concentration the above-mentioned ratio changes in favor of the NNN dipoles. In our ionic thermocurrent experiments on the system  $\text{Ba}_{1-x}\text{La}_x\text{F}_{2+x}$  we have observed three peaks: a weak one at about 137 K, which is associated with NN dipoles; a stronger one at about 190 K, which is due to NNN complexes; and a very strong one, which shifts to lower temperatures with increasing values of  $x$ . This strong peak is due to space charges which are produced by the polarizing field. The conductivity mechanism will be discussed in terms of the two-jump mechanism proposed in an earlier paper. In the range of low concentrations the eventual role of monovalent cations and oxide impurities is discussed. In order to obtain more information about the defect structure of the solid solutions  $\text{Ba}_{1-x}\text{La}_x\text{F}_{2+x}$ , we have investigated the development of the linewidth of the different resonances observed for trigonal  $\text{Gd}^{3+}$  probes which had been introduced into the samples. The observations have been analyzed, and it has been concluded that the  $\text{Gd}^{3+}$  probes are perturbed by distant  $\text{La}^{3+}\text{-F}_i^-$  dipoles. The broadening of the EPR lines will be calculated using a statistical model; the electrostatic interactions of the dipoles are found to shift the fine lines of the  $\text{Gd}^{3+}$  probes. The theoretical model employed here is found to give reasonable agreement with the experimental results.

## I. INTRODUCTION

Solid solutions consisting of  $\text{AF}_2$  and  $\text{RF}_3$  (where  $A$  is an alkaline-earth and  $R$  is a rare-earth ion) form an interesting group of materials. It is possible to prepare single crystals of mixtures of alkaline-earth fluorides and rare-earth fluorides ( $\text{A}_{1-x}\text{R}_x\text{F}_{2+x}$ ) for values of  $x$  up to 0.4–0.5 without losing the fluorite lattice structure. In recent literature<sup>1–4</sup> the structure of these solid solutions has been studied in some detail and it has been found that dipolar defects occur in slightly doped materials. These dipoles consist of a substitutional  $\text{R}^{3+}$  ion and an interstitial fluoride ion at a nearest-neighbor (NN) or a next-nearest-neighbor (NNN) position. A schematic presentation of these two complexes has been given in Fig. 1. It has been shown that in some materials only NN or NNN dipoles occur whereas in other materials both types of dipoles can be observed.<sup>5,6</sup> Because these two different complexes can be transformed very easily into each other we know that the energies of formation of these complexes are about the same. In an earlier paper on  $\text{Sr}_{1-x}\text{Gd}_x\text{F}_{2+x}$  we have shown that the energy difference of the two different defects is only a few hundredths of an eV.<sup>7</sup>

In some  $\text{A}_{1-x}\text{R}_x\text{F}_{2+x}$  materials there is a relatively strong tendency of the dipolar defects to form clusters. This has been observed very clearly by Wright and co-

workers<sup>8–10</sup> using high-resolution spectroscopy. Moore and Wright<sup>11</sup> have found different types of  $\text{Er}^{3+}$  clusters in  $\text{CaF}_2\text{:Er}$  by means of selective laser spectroscopy. Among the centers present these authors found dimers and even trimers.

Recently, important work on clustering phenomena in solid solutions  $\text{Ca}_{1-x}\text{R}_x\text{F}_{2+x}$  has been carried out by Cor-

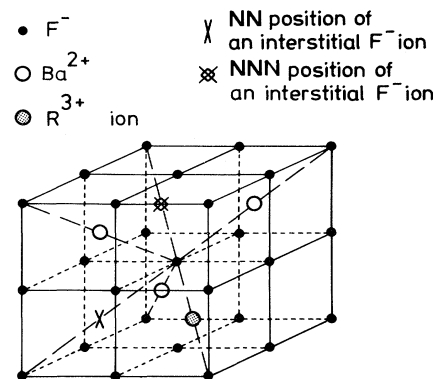


FIG. 1. Three-dimensional schematic representation of the  $\text{BaF}_2$  lattice containing an NN and an NNN dipole, consisting of a substitutional  $\text{R}^{3+}$  impurity and an interstitial fluoride ion.

ish *et al.*,<sup>12</sup> who have calculated the energies of different types of defects. These authors have found that in some solid solutions it is energetically advantageous to form dimers with an additional interstitial fluoride ion. This has also been suggested by Wintersgill *et al.*<sup>13</sup> on the basis of their results for the activation volume of what these authors refer to as the *R* IV relaxation peak.

It is, however, quite probable that the formation of coagulates depends upon three parameters: the radius of the divalent cation of the host crystal, the radius of the trivalent impurity, and the magnitude of the relaxations necessary to accommodate the interstitial fluoride ion in the neighborhood of the impurity. We have found that it is quite probable that the systems  $\text{Sr}_{1-x}\text{Dy}_x\text{F}_{2+x}$ ,  $\text{Sr}_{1-x}\text{Er}_x\text{F}_{2+x}$ , and  $\text{Sr}_{1-x}\text{Yb}_x\text{F}_{2+x}$  show extensive clustering at relatively low  $R^{3+}$  concentrations.<sup>14,15</sup> In other materials, however, such as  $\text{Sr}_{1-x}\text{La}_x\text{F}_{2+x}$ ,  $\text{Sr}_{1-x}\text{Ce}_x\text{F}_{2+x}$ , and  $\text{Sr}_{1-x}\text{Nd}_x\text{F}_{2+x}$  clustering plays a minor role even at high  $R^{3+}$  concentrations.<sup>16,17</sup>

From comparison of the behavior of the dielectric properties of the solid solutions studied in this paper ( $\text{Ba}_{1-x}\text{La}_x\text{F}_{2+x}$ ) with the above-mentioned properties, we will conclude that in the materials investigated here clustering does not play an essential role. Also the results obtained from EPR experiments on the solid solutions  $\text{Ba}_{1-x}\text{La}_x\text{F}_{2+x}$  slightly doped with  $\text{GdF}_3$  support the conclusion that  $\text{La}^{3+}\text{-F}_i^-$  dipoles do not show extensive clustering. It appears that it is not possible to describe the different solid solutions with one definite structure. We have observed only one dominant EPR signal which has been connected with trigonal dipoles of the NNN type. A weak signal observed with the very sensitive *Q*-band spectrometer is probably due to low-symmetry  $\text{Gd}^{3+}$  centers. Clustering is not excluded, but from the intensity of the spectra we find that it is a relatively unimportant phenomenon for the solid solution studied in the present paper. We will see from our results that this conclusion holds at least up to concentrations of a few mol %.

The defect structure determines both the dielectric properties and the ionic conductivity of the material. Therefore, the conclusion that dipoles are the dominant defects has implications for these physical properties. The conductivity is discussed in terms of a percolation-type model in which the dipoles play a decisive role. The NN and NNN dipoles reorient very rapidly as compared to the jumping behavior of free-anion interstitials. This has led us to a model for the solid solution. We assume that it consists of a heterogeneous mixture of two different materials. Firstly, we have the insulating host material in which free-anion interstitials move relatively slowly, and secondly, there is a conducting material that consists of the ions within the sphere of a reorienting dipole. This sphere has a fairly large volume; it is about 11 times the volume of one  $\text{BaF}_2$  molecule. For sufficiently high concentrations of the La impurities the spheres overlap and the interstitial fluoride ions can jump from one dipole system to another one. If the volume fraction of the "conducting" spheres becomes larger than 0.25 percolation conduction occurs. An analysis of the ionic thermocurrent (ITC) results in terms of this model gives results which are quite acceptable.

In the present paper we present EPR and ITC results on solid solutions of the type  $\text{Ba}_{1-x}\text{La}_x\text{F}_{2+x}$ . Apart from the information about the symmetry of the  $\text{Gd}^{3+}$  centers we are able to obtain information concerning the interactions of the  $4f^7$  electron system of the  $\text{Gd}^{3+}$  probes with distant dipolar complexes. We will show that this information supports the above-described defect structure of solid solutions  $\text{Ba}_{1-x}\text{La}_x\text{F}_{2+x}$ . In order to calculate the interactions between distant  $\text{La}^{3+}\text{-F}_i^-$  dipoles and the central  $\text{Gd}^{3+}$  probe we apply the theoretical model given by Bijvank and den Hartog,<sup>18,19</sup> because this method was shown to give good results for ionic crystals.

The ITC results presented in this paper are concerned with the two dipole reorientation peaks associated with NN and NNN dipoles. In contrast with the results reported by Laredo *et al.*<sup>20</sup> we find that the ratio of the concentrations of the two different dipoles changes with the concentration. This effect is ascribed to dipole-dipole interactions. We find that with increasing  $\text{LaF}_3$  concentration the NNN dipoles become more and more dominant. For  $\text{LaF}_3$  concentrations of about  $10^{-4}$  we find, for the ratio  $c_{\text{NNN}}/c_{\text{NN}}$ , a value of 1, whereas for a concentration of about  $10^{-2}$  this value is 2.

In addition, we have investigated the behavior of a depolarization peak which we have connected with space charges. In contrast with the results on the dipole reorientation peaks we find that the space-charge band shifts gradually to lower temperatures with increasing  $\text{LaF}_3$  concentrations. This shift is due to changes of the conduction mechanism, which will be discussed in this paper in some detail. We have found that for low  $\text{LaF}_3$  concentrations the conductivity by anion vacancies is significant. In these samples the vacancies, which may be associated with monovalent cation impurities or divalent anions (such as oxygen), dominate the conduction process.

## II. EXPERIMENTAL PROCEDURES

The single crystals employed for this investigation have been prepared with a modified Bridgman setup, which has been described in some detail before.<sup>5,21</sup> The mixtures of  $\text{BaF}_2$ ,  $\text{LaF}_3$ , and  $\text{GdF}_3$  were introduced into the furnace system together with 1–2 mol %  $\text{PbF}_2$ , which is used in order to reduce the  $\text{O}^{2-}$  content in the resulting crystalline material.

The EPR experiments were carried out under both *X*- and *Q*-band conditions. The frequencies of the spectrometers are 9.2 and 35.34 GHz, respectively. *Q*-band conditions were used whenever high sensitivity was needed. Especially the weak signals associated with low-symmetry clusters were investigated with the *Q*-band spectrometer. The EPR experiments were carried out at room temperature. The rotational diagrams were analyzed automatically with a data-acquisition system consisting of a Varian E 901 interface, a Hewlett-Packard HP-9835 desk-top computer, a HP floppy disk system, and a HP-7225 A plotter. A program developed for this system has been used to determine the peak positions as a function of the rotation angle. In addition to this the plotter provides us immediately after the experiment with the rotational diagram.

From some selected EPR transitions the peak-to-peak

widths of the first derivative signal have been determined. The behavior of the additional contribution to the linewidth due to electrostatic interactions with distant trigonal electrical dipoles has been determined assuming that the distribution of crystal fields leads to a Gaussian line shape.

The ITC experiments were carried out with a setup, which has been described in our earlier papers.<sup>5,6</sup> Part of the experiments has been done with a slightly modified setup. In the latter experiments the setup is computer controlled and the data are collected on a floppy disk or a tape. The temperature is increased linearly with time; this leads to improved results, which are more suitable for a theoretical analysis. We note that an approximation in the description of the ITC peak as given by van Weperen *et al.*<sup>22</sup> is that the temperature is a linear function of time during the experiment. It is expected therefore that in the future it will be possible to carry out more accurate analyses of the experimental results, providing us with more precise values for the relaxation parameters and the strength of the dipole-dipole interactions.

The concentration  $x$  of the La ions in the  $\text{BaF}_2$  lattice has been determined with x-ray fluorescence. This method gives reliable results for  $x \geq 0.01$ . A complicating factor for the system  $\text{Ba}_{1-x}\text{La}_x\text{F}_{2+x}$  is that the most suitable La emission in the x-ray-fluorescence spectrum is quite close to an intense Ba line. As a result the La emission is overwhelmed by that of the Ba line for  $x < 0.01$ . In the concentration range  $0 \leq x \leq 0.01$  we have used the nominal lanthanum concentrations.

### III. EXPERIMENTAL RESULTS

Although the experimental results presented in this paper will be treated to obtain a general picture of the defect

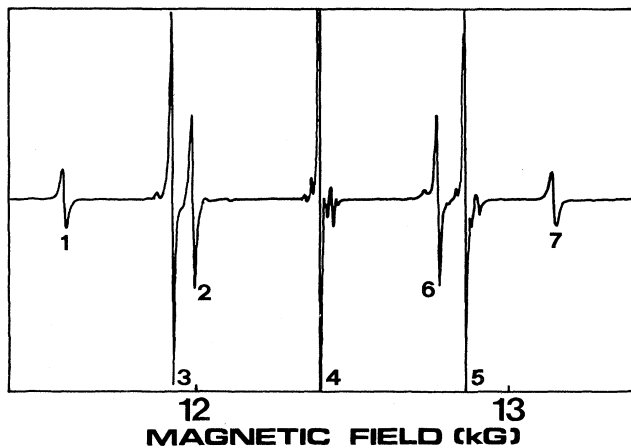


FIG. 2. EPR signal of a  $\text{Ba}_{0.9969}\text{La}_{0.0031}\text{F}_{2.0031}:\text{Gd}^{3+}$  crystal with  $\vec{H}_0 \parallel [100]$  under  $Q$ -band conditions ( $\nu \sim 35$  GHz). Transitions indicated by 1,2,3,...,7 are associated with the  $S_z = -\frac{5}{2} \leftrightarrow -\frac{7}{2}$ ,  $-\frac{3}{2} \leftrightarrow -\frac{5}{2}$ ,  $-\frac{1}{2} \leftrightarrow -\frac{3}{2}$ ,  $\frac{1}{2} \leftrightarrow -\frac{1}{2}$ ,  $\frac{3}{2} \leftrightarrow \frac{1}{2}$ ,  $\frac{5}{2} \leftrightarrow \frac{3}{2}$ , and  $\frac{7}{2} \leftrightarrow \frac{5}{2}$  transition, respectively. As explained in the text the transitions connected with the different orientations of the dipoles coincide because of the specific symmetry of the  $[100]$  direction.

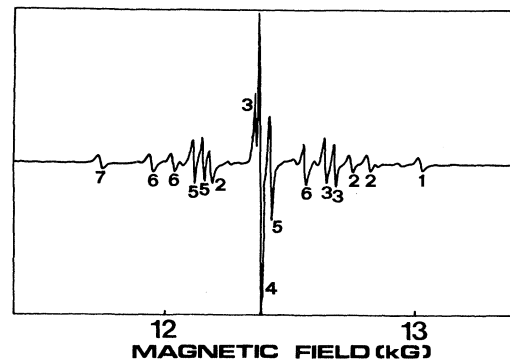


FIG. 3. EPR spectrum of a  $\text{Ba}_{0.9969}\text{La}_{0.0031}\text{F}_{2.0031}:\text{Gd}^{3+}$  crystal with  $\vec{H}_0 \parallel [110]$  under  $Q$ -band conditions. Transitions have been marked in the same way as in Fig. 2.

structure of the materials investigated, we will give the EPR and ITC results in separate sections because of the differences in the nature of these experimental techniques. In addition, the EPR results tell us more about the defect structure whereas the ITC results also give information concerning the conduction mechanism.

#### A. EPR results

In order to study the defect structure of the system  $\text{Ba}_{1-x}\text{La}_x\text{F}_{2+x}$  we have to add to these materials small amounts of  $\text{Gd}^{3+}$  impurities.  $\text{Gd}^{3+}$  acts as a measuring

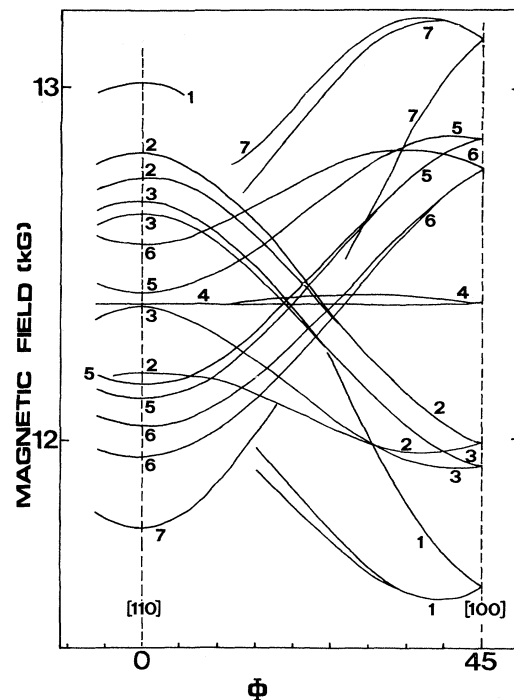


FIG. 4. Behavior of the EPR lines for  $\text{Ba}_{0.9969}\text{La}_{0.0031}\text{F}_{2.0031}:\text{Gd}^{3+}$  during rotation in the  $(001)$  plane. Transitions have been indicated in accordance with the labels shown in Fig. 2.

probe for the crystal-field interactions caused by the ions surrounding the probe. In contrast with the results obtained for EPR experiments on  $Gd^{3+}$  ions in  $Sr_{1-x}La_xF_{2+x}$  we find that in  $Ba_{1-x}La_xF_{2+x}$  the trivalent Gd ions are located predominantly at positions with trigonal axial symmetry.

In Fig. 2 we show an EPR signal obtained for  $Ba_{0.9969}La_{0.0031}F_{2.0031}:Gd^{3+}$  under  $Q$ -band ( $\nu=35.34$  GHz) conditions. The signal with  $\vec{H}_0||[100]$  consists of seven main absorption lines which are associated with the fine transitions  $S_z = -\frac{5}{2} \leftrightarrow -\frac{7}{2}$ ,  $-\frac{3}{2} \leftrightarrow -\frac{5}{2}$ ,  $-\frac{1}{2} \leftrightarrow -\frac{3}{2}$ ,  $\frac{1}{2} \leftrightarrow -\frac{1}{2}$ ,  $\frac{3}{2} \leftrightarrow \frac{1}{2}$ ,  $\frac{5}{2} \leftrightarrow \frac{3}{2}$ , and  $\frac{7}{2} \leftrightarrow \frac{5}{2}$  of four equivalent trigonal dipoles consisting of a trivalent Gd ion and an NNN interstitial fluoride ion. In general, the spectrum consists of  $4 \times 7 = 28$  EPR lines, but along directions of high symmetry this number is reduced because some of the centers are equivalent. This can be seen in Fig. 3 where the EPR signal with  $\vec{H}_0||[110]$  has been shown.

In order to analyze the EPR results completely we present in Fig. 4 the complete rotational diagram of the EPR lines. The diagram has been taken under  $X$ -band conditions, because with these samples which have larger dimensions than the  $Q$ -band samples are easier to orient. We note, however, that, as can be seen from the splitting of the high-field  $\frac{7}{2} \leftrightarrow \frac{5}{2}$  transition there is still some misorientation. From a least-squares-fitting procedure we can obtain the various crystal-field parameters of the spin Hamiltonian

$$\begin{aligned} \mathcal{H}_{\text{trig}} = & g\mu_B \vec{H}_0 \cdot \vec{S} + B_2^0 O_2^0 + B_4^0 O_4^0 + B_4^3 O_4^3 \\ & + B_6^0 O_6^0 + B_6^3 O_6^3 + B_6^6 O_6^6. \end{aligned} \quad (1)$$

The crystal-field parameters  $B_i^m$  have been determined for both the  $X$ -band and  $Q$ -band results; they have been compiled in Table I. We observe that the two sets of parameters agree quite closely. It should be noted that the accuracy of the parameters  $B_2^0$ ,  $B_4^0$ , and  $B_4^3$  is about 0.4%; the relative error in  $B_6^0$  is 15% and for  $B_6^3$  and  $B_6^6$  the corresponding values are about 50%. With regard to the  $B_i^m$  parameters we note that their effects on the observed line positions are small. The values obtained from the  $X$ - and  $Q$ -band experiments agree rather closely with those reported by Boatner *et al.*<sup>23</sup>

The EPR spectrum associated with the trigonal complexes is the dominant one. Apart from this signal we have observed in our  $Q$ -band spectra weak lines due to  $Gd^{3+}$  ions with low point symmetry. We have not investigated these lines in great detail, but the rotational diagram obtained for the extra lines indicate that the principal axes of the centers associated with the lines cannot be along the crystallographic [100] or [110] axis. The [111] axis cannot be excluded.

We have observed that the additional low-symmetry



FIG. 5. Effect of broadening due to electrostatic interactions between distant  $La^{3+}-F_i^-$  dipoles and the  $Gd^{3+}$  probes on the  $\frac{5}{2} \leftrightarrow \frac{3}{2}$  and  $\frac{3}{2} \leftrightarrow \frac{1}{2}$  transitions. Apart from the  $Gd^{3+}$  probes the samples contain 0.007 or 0.70 mol%  $LaF_3$ . Crystals were oriented with  $\vec{H}_0||[110]$  and the experiments have been carried out under  $X$ -band conditions ( $\nu \sim 9.2$  GHz).

signals do not increase drastically with increasing La concentrations, indicating that if these signals are associated with some kind of clusters with more than one trivalent  $R$  ion, clustering does not play an important role in these materials. This is in contrast with results reported in the literature on various similar solid solutions of the type  $AF_2:RF_3$ . In different solid solutions extensive clustering has been observed with very sensitive spectroscopic techniques<sup>8-10</sup> and with diffraction methods.<sup>24</sup> In addition, calculations for various systems have shown that the geometry of the clusters can be predicted quite well.<sup>25</sup>

An important consequence of the presence of the  $La^{3+}$  impurities in the materials is the broadening of the EPR lines. From the rotational diagram and the spin Hamiltonian as given in Eq. (1) we know for each of the observed EPR lines the nature of the transition (i.e., the spin quantum numbers involved). In order to study the broadening of the EPR lines we should avoid taking spectra with the magnetic field direction along crystal directions of high symmetry (e.g., [100]) because of eventual overlaps of the EPR lines, which disturb the results. For

TABLE I. Spin-Hamiltonian parameters of  $Gd^{3+}$  in  $Ba_{1-x}La_xF_{2+x}$  ( $B_i^m$  in G).

	$g$	$B_2^0$	$B_4^0$	$B_4^3$	$B_6^0$	$B_6^3$	$B_6^6$
$Q$ band	1.9902	-45.2	0.41	-11.42	$-2.0 \times 10^{-4}$	$72 \times 10^{-4}$	$22 \times 10^{-4}$
$X$ band	1.9916	-45.4	0.41	-11.50	$-2.0 \times 10^{-4}$	$72 \times 10^{-4}$	$22 \times 10^{-4}$

our purposes we found it useful to study the broadening effect of some transitions with  $\vec{H}_0$  close to [110].

In Fig. 5 we show some typical results of our investigations of the broadening effects. We note that we have only given a few examples and that we have studied many different transitions. From Fig. 5 we can see first that the width of the EPR lines of the sample doped with 0.70 mol%  $\text{LaF}_3$  are larger than those of the corresponding lines in the sample containing 0.007 mol%  $\text{LaF}_3$ . In addition, it can be seen that the broadening of the  $\frac{5}{2} \leftrightarrow \frac{3}{2}$  transition is larger than for the  $\frac{3}{2} \leftrightarrow \frac{1}{2}$  transition. In Fig. 6 we give the behavior of the  $\frac{5}{2} \leftrightarrow \frac{3}{2}$  transition as a function of the concentration and we observe that, taking into account the scatter of the experimental data, the results can be described fairly well with a linear function of the concentration  $x$ .

An important feature of our results is that the extra contribution to the linewidth, which is associated with the presence of the trivalent La ions, depends very strongly upon the nature of the transition. We found that the transition  $S_Z = +\frac{1}{2} \leftrightarrow -\frac{1}{2}$  is not affected by the La impurities. The extra contributions to the linewidth for the transitions  $\frac{3}{2} \leftrightarrow \frac{1}{2}$ ,  $\frac{5}{2} \leftrightarrow \frac{3}{2}$ , and  $\frac{7}{2} \leftrightarrow \frac{5}{2}$  have a ratio of approximately 1:2:3. This result agrees well with the observation made during similar experiments on crystals of the type  $\text{Sr}_{1-x}\text{La}_x\text{F}_{2+x}$  and  $\text{Ca}_{1-x}\text{La}_x\text{F}_{2+x}$ .<sup>26</sup> The present results indicate that, just as for the previously studied materials, the extra contribution to the linewidth is due to additional terms in the crystal-field Hamiltonian. Because of the observed ratio these extra terms should be of the type

$$\mathcal{H}_{\text{pert}} = \sum_m B_2^{m*} O_2^m. \quad (2)$$

If higher-degree crystal-field terms would contribute to the extra linewidths of the EPR transitions the ratio would significantly deviate from the observed one.

### B. ITC results

In an ITC experiment on  $\text{Ba}_{1-x}\text{La}_x\text{F}_{2+x}$  we observe in general three depolarization peaks: a low-temperature peak at about 140 K, which is connected with tetragonal complexes consisting of a  $\text{La}^{3+}$  ion and an interstitial

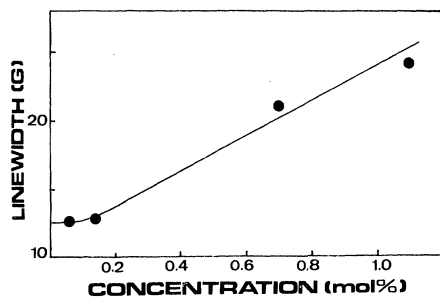


FIG. 6. Behavior of the extra broadening of the  $\frac{5}{2} \leftrightarrow \frac{3}{2}$  transition due to interactions between the  $\text{Gd}^{3+}$  ion and distant  $\text{La}^{3+}-\text{F}_i^-$  dipoles as a function of the La concentration. For La concentrations larger than 0.1 mol% the width of this EPR line increases linearly with the concentration.

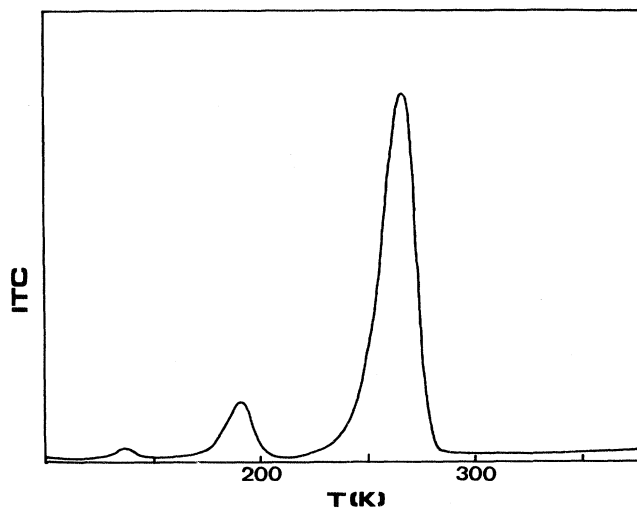


FIG. 7. ITC curve observed for a  $\text{BaF}_2$  sample doped with about 0.1 mol%  $\text{LaF}_3$ . Sample was polarized for 5 min with an electric field of 4 kV/mm at a temperature of 400 K.

fluoride ion located at a NN position (NN dipole); the second peak at about 190 K, which is due to a trigonal dipolar complex with an interstitial fluoride ion at a NNN position (NNN dipole); the third peak, which is much more intense than the other ITC peaks, is connected with the development of space-charge clouds opposite to the electrodes. A characteristic result of an ITC experiment has been given in Fig. 7. We can see that the low-temperature peak, which will be referred to as the LT peak, is weaker than the peak at 190 K, which will be called the medium-temperature (MT) peak.

We have analyzed the ITC peaks with the ITC formula derived by van Weperen, Lenting, Bijvank, and den Hartog<sup>22</sup> and we found for the activation energy of the MT peak an average value of 0.57 eV; for  $\tau_0$  we have derived a value of  $1.5 \times 10^{-13}$  sec. In addition, we found just as van Weperen *et al.*<sup>22</sup> that the broadening of the activation energy is a linear function of the concentration as long as the concentration  $x$  is in the range  $0 \leq x \leq 5 \times 10^{-3}$ . For values of  $x$  larger than  $5 \times 10^{-3}$  the approximations made by van Weperen *et al.*<sup>22</sup> are no longer valid.

We have determined the total amount of displaced

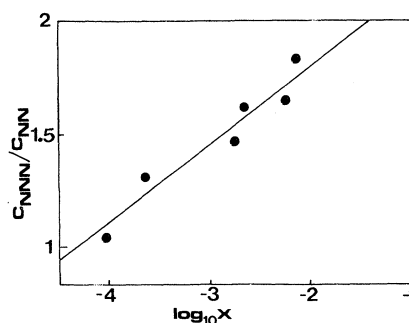


FIG. 8. Behavior of the concentration ratio of NNN and NN dipoles as a function of the total amount of  $\text{LaF}_3$  introduced into the  $\text{BaF}_2$  crystal.

charge at the electrodes for both the LT and the MT peak in a considerable range of concentrations ( $0 \leq x \leq 0.01$ ) and we found that the relative concentration of tetragonal complexes (associated with the LT peak) decreases while the trigonal center becomes more and more the dominant center. In Fig. 8 we show a review of our experimental results, where we can see that the concentration ratio of the trigonal and the tetragonal dipoles increases by approximately a factor of 2. This behavior has also been observed for  $\text{Sr}_{1-x}\text{Gd}_x\text{F}_{2+x}$  in both EPR and ITC experiments by Aalbers and den Hartog.<sup>7</sup> These authors have explained the variation of the concentration ratio in terms of dipole-dipole interactions. We note that in the samples studied in the present paper the concentrations of the trivalent impurities are about the same as those in the samples investigated by Aalbers and den Hartog; thus the effects of dipole-dipole interactions will be about the same.

den Hartog and Langevoort<sup>27</sup> have studied in a recent paper the behavior of the space-charge-relaxation band as a function of the concentration of trivalent La impurities. In the present study we have paid extra attention to the range of low concentrations. In Fig. 9 the behavior of the position of the space-charge-relaxation peak has been shown. In contrast with the results obtained for  $\text{Sr}_{1-x}\text{Nd}_x\text{F}_{2+x}$  and  $\text{Sr}_{1-x}\text{La}_x\text{F}_{2+x}$  we see that in  $\text{Ba}_{1-x}\text{La}_x\text{F}_{2+x}$  the value of  $T_{\text{max}}$  keeps increasing in the low-concentration range. Between 1 and 10 mol. %  $\text{LaF}_3$  the position of the high-temperature (HT) band shifts very rapidly with increasing concentration to lower temperatures. At very high concentrations the space-charge-relaxation peak is located at the same temperature as the MT (NNN) band in slightly doped materials.

In order to obtain more information about the jump mechanisms giving rise to the space-charge-relaxation peak we have studied some  $\text{BaF}_2$  crystals doped with small amounts of NaF. In these materials one expects that the ionic conductivity is controlled by vacancy jumps. In Fig. 10 we show the ITC result of a  $\text{BaF}_2$  crystal doped with 0.15 mol % NaF. The space-charge-relaxation band is located at 345 K, i.e., at significantly higher tempera-

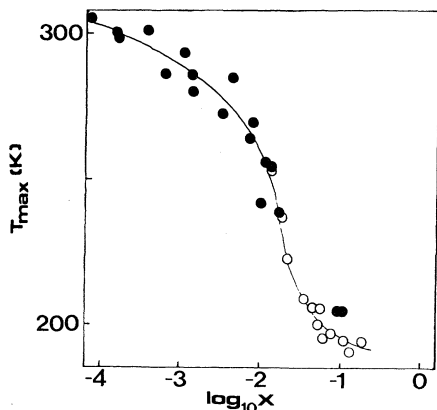


FIG. 9. Behavior of the position of the space-charge-relaxation (HT) peak as a function of the concentration of  $\text{La}^{3+}$  ions in the samples.

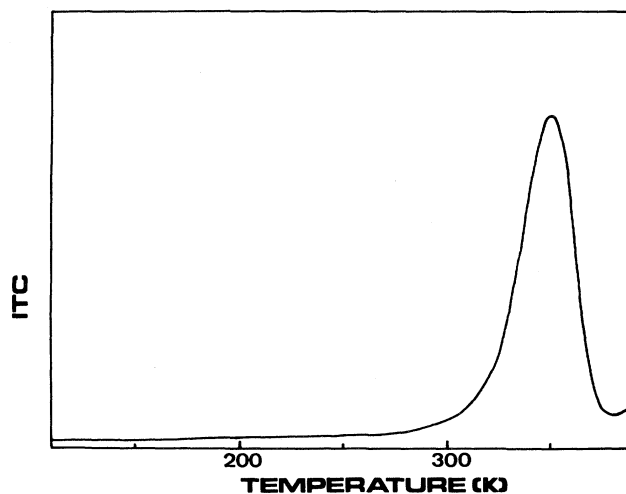


FIG. 10. ITC curve observed for a  $\text{BaF}_2$  sample doped with 0.15 mol % NaF. Sample was polarized for 5 min with an electric field of 4 kV/mm at a temperature of 400 K.

tures than in  $\text{BaF}_2$  doped very slightly with  $\text{LaF}_3$ . Although we did not study the relation between the position of the space-charge-relaxation peak and the Na concentration in detail, we observed that also for the system  $\text{Ba}_{1-x}\text{Na}_x\text{F}_{2-x}$  the value of  $T_{\text{max}}$  decreases with increasing Na concentrations. It is quite probable that in the Na-doped crystals the space-charge-relaxation peak occurs as a result of the motion of anion vacancies. Comparing the position of the HT band in La- and Na-doped crystals, we conclude that vacancies in  $\text{BaF}_2$  are less mobile than interstitial fluoride ions. With this conclusion it is possible to explain the above-mentioned observation that in the low-concentration region the value of  $T_{\text{max}}$  of the HT band increases with decreasing La concentration. We assume that in undoped  $\text{BaF}_2$  both alkali ions and oxygen impurities are present, which give rise to anion vacancies. In  $\text{BaF}_2$  crystals which are slightly doped with La ions the vacancies outnumber the interstitial fluoride ions. In this situation the space-charge-relaxation band is governed by the motion of anion vacancies, i.e., at very low La concentrations the HT-band position will tend to a temperature of 345 K.

#### IV. DISCUSSION

The results of our ITC and EPR experiments show that in cubic  $\text{Ba}_{1-x}\text{La}_x\text{F}_{2+x}$  and in  $\text{Ba}_{1-x-y}\text{La}_x\text{Gd}_y\text{F}_{2+x+y}$  the trigonal dipoles consisting of a trivalent R ion and an interstitial fluoride ion are the predominant defects. In  $\text{Ba}_{1-x}\text{La}_x\text{F}_{2+x}$  there are also tetragonal dipoles, but with increasing values of  $x$  the trigonal complexes become more and more dominant over the tetragonal complexes. This variation of the concentration ratio of trigonal and tetragonal dipoles can be understood by taking into account the interaction between the dipoles. In addition, we note that the difference between the formation energies  $\Delta E$  of trigonal and tetragonal is very small (of the order of  $10^{-2}$  eV).

Assuming that the formation energies of the dipolar de-

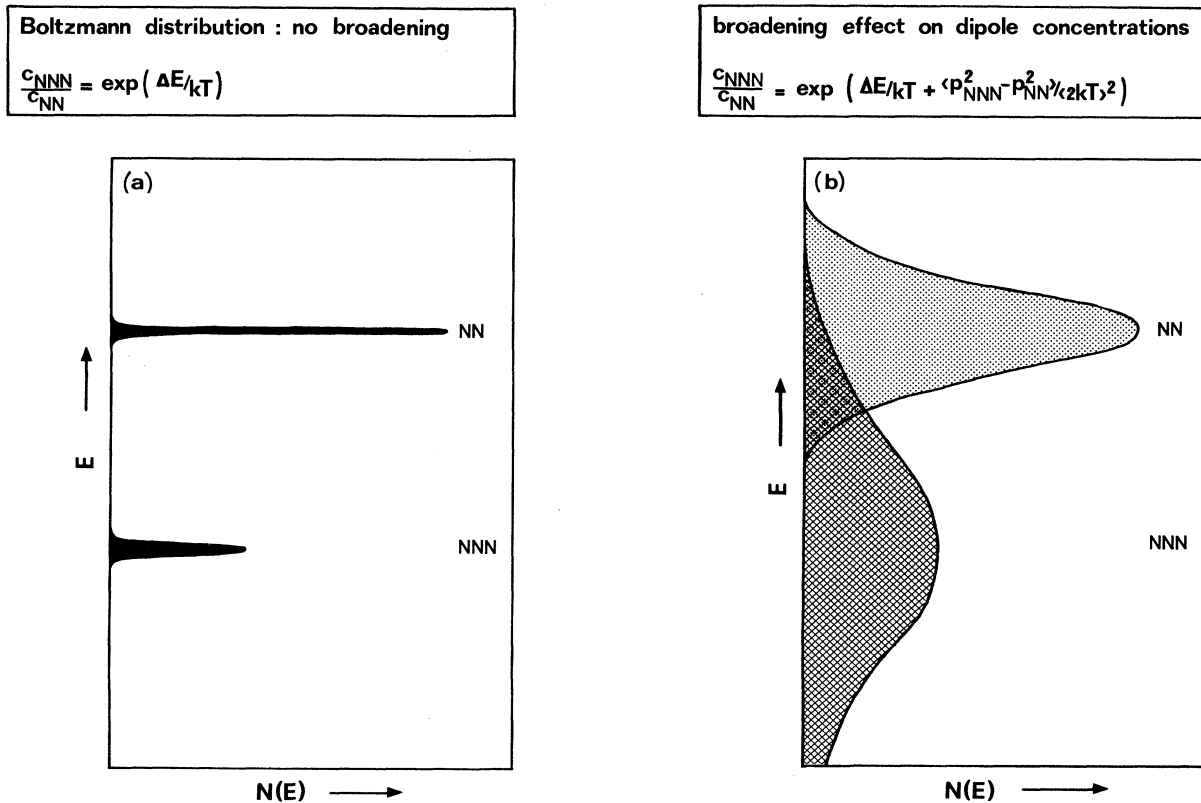


FIG. 11. (a) Distributions of dipole energies for both tetragonal and trigonal dipoles. Here the widths of the distribution functions are small as compared with the separation between the peaks. (b) Distributions of dipole energies for both tetragonal and trigonal dipoles. Here the widths of the distribution functions are of the same order of magnitude as the separation between the two peaks.

fects no longer have unique values as a result of dipole-dipole interaction, and assuming that these formation energies can be described by Gaussian distribution functions, we can understand the observed behavior. In Fig. 11 we show two extreme situations: In Fig. 11(a) the dipole-dipole interaction is weak and as a result the ratio of the concentrations of the trigonal and tetragonal dipoles is determined by the Boltzmann relation

$$c_{\text{trig}}/c_{\text{tetrag}} = e^{\Delta E/kT}. \quad (3)$$

In Fig. 11(b) the ratio of the trigonal and tetragonal dipoles will deviate from the Boltzmann factor because the dipole-dipole interactions will result in an overlap of the distribution functions. Aalbers and den Hartog<sup>7</sup> have derived for the ratio of the trigonal and tetragonal dipoles

$$\frac{c_{\text{trig}}}{c_{\text{tetrag}}} = \exp \left[ \left( \Delta E + \frac{p_{\text{trig}}^2 - p_{\text{tetrag}}^2}{4kT} \right) \frac{1}{kT} \right]. \quad (4)$$

In (4),  $p_{\text{trig}}$  and  $p_{\text{tetrag}}$  are the widths of the distribution functions in Fig. 11(b). It is clear that it is possible to observe the above-mentioned variations only if  $\Delta E$  and  $p$  are of the same order of magnitude as  $kT$  ( $\sim 10^{-2}$  eV). From the observed behavior of the concentration ratio we estimate the value of  $\Delta E$  to be  $0-10^{-2}$  eV. In addition, we find for  $p_{\text{trig}}$  a value of  $3 \times 10^{-2}$  eV at a La concentration of 1 mol %. In this calculation we have neglected the ef-

fect of  $p_{\text{tetrag}}$  because we expect that, as a result of the rather small value of the dipole strength of the tetragonal dipoles (see also Aalbers and den Hartog<sup>7</sup>),  $p_{\text{tetrag}}^2$  is much smaller than  $p_{\text{trig}}^2$ .

From our EPR experiments we have found that for the complexes involving trivalent gadolinium the trigonal centers are much more dominant than for complexes with La<sup>3+</sup>. This is probably due to the difference in the ionic radii of Gd<sup>3+</sup> and La<sup>3+</sup>. We note in this regard that also in the series Sr<sub>1-x</sub>R<sub>x</sub>F<sub>2+x</sub> the trigonal dipole becomes more stable for the heavier R ions (i.e., decreasing R<sup>3+</sup> radius). In Sr<sub>1-x</sub>La<sub>x</sub>F<sub>2+x</sub> the tetragonal dipoles are the dominant ones, whereas in Sr<sub>1-x</sub>Lu<sub>x</sub>F<sub>2+x</sub> the trigonal complexes are dominant.<sup>5</sup> In SrF<sub>2</sub> doped with small amounts of GdF<sub>3</sub>, TbF<sub>3</sub>, or HoF<sub>3</sub> both types of dipoles have been observed.

Apart from the trigonal Gd<sup>3+</sup>-F<sub>i</sub><sup>-</sup> centers we have also observed at least one other type of Gd<sup>3+</sup> center. It is possible that this center is a cluster containing two trivalent ions, i.e., one Gd<sup>3+</sup> and one La<sup>3+</sup>; we have, however, not observed drastic increases in the extra EPR signal with increasing La<sup>3+</sup> concentrations. Also at high La<sup>3+</sup> concentrations the predominant Gd<sup>3+</sup> center in Ba<sub>1-x-y</sub>La<sub>x</sub>Gd<sub>y</sub>F<sub>2+x+y</sub> is the trigonal dipole. We conclude from this observation that if there is clustering in the crystals, the Gd<sup>3+</sup> impurities do not participate in the clustering process. Unfortunately, it is not possible to ob-

tain direct information concerning the point-group symmetry of the  $\text{La}^{3+}$  centers with EPR because the ion under consideration is not paramagnetic. With the method employed here, however, we can obtain indirect information about the defect structure of the system  $\text{Ba}_{1-x}\text{La}_x\text{F}_{2+x}$  by analyzing the behavior of the linewidth of the EPR transitions associated with trivalent Gd probes, which has been introduced into the crystals during crystal growth.

In an earlier paper on  $\text{Ca}_{1-x-y}\text{La}_x\text{Gd}_y\text{F}_{2+x+y}$  and  $\text{Sr}_{1-x-y}\text{La}_x\text{Gd}_y\text{F}_{2+x+y}$  ( $x \gg y$ ) one of the authors has given a treatment of the broadening of the fine transitions of trivalent gadolinium impurities due to interactions with distant electrical dipoles. In the present case we can apply a similar analysis; there are, however, a few minor differences. Firstly, we should realize that in the materials under consideration the major interactions are due to trigonal dipoles, and secondly, as we have mentioned before, the EPR lines were recorded not with  $\vec{H}_0 \parallel [100]$ , because in that case the lines may be broadened by a small misalignment, but instead the spectra were analyzed for  $\vec{H}_0 \parallel [110]$ .

Using the relationship between the electrostatic crystal-potential and the crystal-field parameter of the second degree derived by Bijvank and den Hartog,<sup>18,19</sup> we find for the contribution, in units of G,

$$B_2^{0*} = 10.2 \times 10^{18} \frac{e}{16\pi\epsilon_0} \left[ \frac{3Z_{\text{La}}^2 - R_{\text{La}}^2}{R_{\text{La}}^5} - \frac{3Z_{\text{Fi}}^2 - R_{\text{Fi}}^2}{R_{\text{Fi}}^5} \right]. \quad (5)$$

For the other  $B_2^m$  parameters we can write down similar expressions. In (5)  $Z_{\text{La}}$ ,  $R_{\text{La}}$ ,  $Z_{\text{Fi}}$ , and  $R_{\text{Fi}}$  are the Z coordinate and the distance to the central Gd nucleus of the  $\text{La}^{3+}$  ion and the interstitial fluoride ion, respectively. The  $\text{La}^{3+}$  impurities and interstitial fluoride ions are assumed to form trigonal dipoles. In order to calculate the effect of these dipoles on the EPR lines of the  $\text{Gd}^{3+}\text{-F}_i^-$  dipoles we draw a sphere with the  $\text{Gd}^{3+}$  probe at the center. The radius of the sphere is chosen such that there is one  $\text{La}^{3+}\text{-F}_i^-$  dipole within the sphere. As a consequence the radius of the sphere depends upon the concentration of  $\text{La}^{3+}\text{-F}_i^-$  dipoles in the crystal. It is assumed that the probability of the  $\text{La}^{3+}$  impurity to occupy any of the substitutional  $\text{Ba}^{2+}$  sites is the same; i.e., the distribution of the  $\text{La}^{3+}\text{-F}_i^-$  dipoles is a purely statistical one. In addition, we assume that the distribution of the dipole orientations (i.e., the position of the interstitial fluoride ion connected with the  $\text{La}^{3+}$  impurity) is also statistical. From the calculations using Eq. (5) and the corresponding equations for the other  $B_2^{m*}$  parameters, and taking into account the contributions from all possible dipole positions and orientations within the sphere, we obtain a histogram showing the distribution of the shifts of the EPR lines divided by 3, 6, or 9, depending on the fine line, which is considered. The shifts of the  $\pm \frac{1}{2} \leftrightarrow \pm \frac{3}{2}$ ,  $\pm \frac{3}{2} \leftrightarrow \pm \frac{5}{2}$ , and  $\pm \frac{5}{2} \leftrightarrow \pm \frac{7}{2}$  transitions are divided by 3, 6, and 9, respectively. In Fig. 12 we present some typical results for different  $\text{La}^{3+}$  concentrations. We emphasize

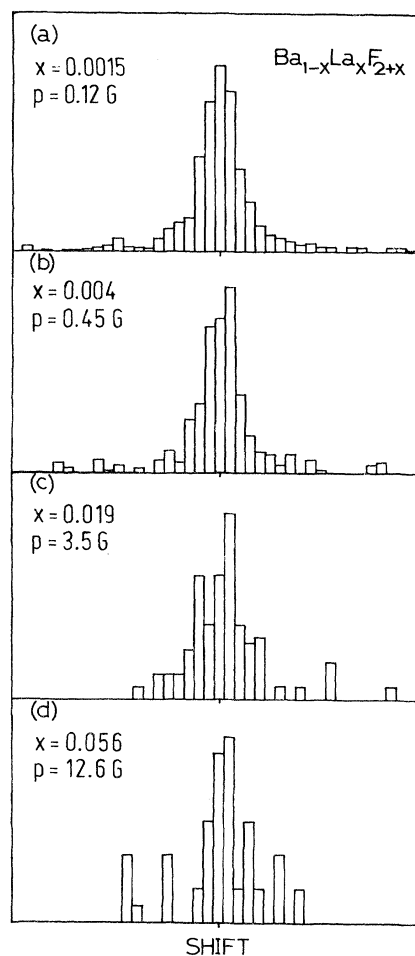


FIG. 12. Theoretically calculated histograms showing the distributions of the normalized shifts of the EPR lines for different concentrations  $x$ . Broadening parameter  $p$  calculated from these histograms is related with the broadening of the EPR lines as described by den Hartog (Ref. 23). In order to obtain the distributions of the shifts of the  $\pm \frac{5}{2} \leftrightarrow \pm \frac{1}{2}$ ,  $\pm \frac{3}{2} \leftrightarrow \pm \frac{5}{2}$ , and  $\pm \frac{1}{2} \leftrightarrow \pm \frac{3}{2}$  transitions the results shown in this figure should be multiplied by 9, 6, and 3, respectively.

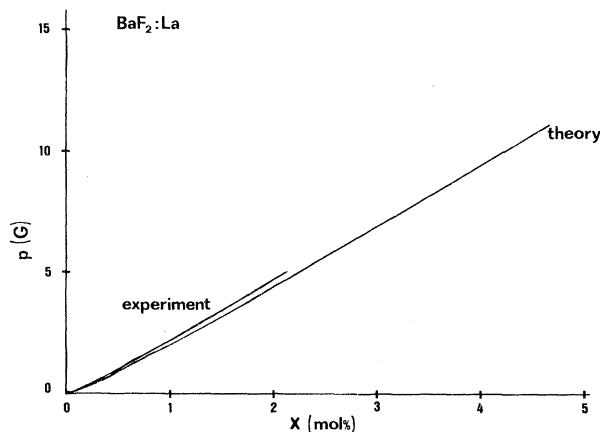


FIG. 13. Comparison of the theoretically calculated and the experimentally observed broadening parameters  $p$  as a function of the  $\text{LaF}_3$  concentration.

that in the different histograms we have taken different step sizes; therefore, the widths of the distributions are different although they look similar. It should be noted also that for high concentrations the sphere becomes quite small and consequently the statistical fluctuations in the histogram are considerable.

A review of the theoretically calculated widths and a comparison between theory and experiment has been presented in Fig. 13. It can be seen that there is fair agreement between theory and experiment. It appears that the experimental broadening is slightly larger than the theoretically observed broadening. With regard to this problem we must make two remarks. First, we know that the relation between the electrostatic crystal-field potential and the splitting of the magnetic energy levels is not well established yet. Bijvank and den Hartog<sup>18</sup> have found that the proportionality factor  $10.2 \times 10^8$  appearing in Eq. (5) may in fact range between  $10-15 \times 10^{18}$ . Another uncertainty is connected with the fact that we have taken into account electrostatic interactions only. If elastic interactions play a role also, it would probably increase the theoretical result. In conclusion we can say that the results obtained here are quite reasonable. From the behavior of the additional contributions to the linewidth as a function of the La concentration we conclude that it is highly improbable that clustering of the La<sup>3+</sup>-F<sub>i</sub><sup>-</sup> dipoles is important in the solid solutions studied in this paper. If clustering would be extensive a drastic reduction of the extra linewidth would occur, because clusters give rise to short-range quadrupole interactions; in addition, the number of defects is reduced, consequently the average distance between the defects increases. Another possibility is the formation of gettered 2:2:2 clusters as proposed by Wintersgill *et al.*<sup>13</sup> and Corish *et al.*<sup>12</sup> or linear of L-shaped clusters which have also been discussed by Corish *et al.*<sup>12</sup> This type of clustering provides us with appreciable numbers of monopoles instead of quadrupoles, etc. These monopoles interact relatively strongly with the 4f<sup>7</sup>-electron system at large distances. If appreciable clustering of this type occurs in our samples the widths of the EPR lines will be significantly larger than expected for a system with only dipolar complexes. We note, however, that we have not observed important additional relaxation peaks, which can be associated with these clusters. In Ba<sub>1-x</sub>La<sub>x</sub>F<sub>2+x</sub> we have observed an additional relaxation peak at slightly lower temperatures than the NN dipole peak, but this peak is *very weak*. If this band is associated with either of the clusters containing an additional interstitial F<sup>-</sup> ion, we conclude that the clustering of this type is unimportant.

The ITC results point into the same direction. Clustering of La<sup>3+</sup>-F<sub>i</sub><sup>-</sup> dipoles is unimportant in BaF<sub>2</sub>. Recently, we have investigated some solid solutions of the type A<sub>1-x</sub>R<sub>x</sub>F<sub>2+x</sub> in which extensive clustering occurs. In these materials we observed, for concentrations  $x \geq 0.5\%$ , a decrease in the number of dipolar defects. In addition, we have observed a complicated behavior of the space-charge-relaxation band as a function of the concentration of trivalent impurities.<sup>14,15</sup> In the low-concentration range the value of  $T_{\max}$  of the HT band decreases with increasing concentration. At R<sup>3+</sup> concentrations of about 0.5

mol %  $T_{\max}$  reaches a minimum value, and for concentrations between 0.5 and 5 mol %, the value of  $T_{\max}$  increases with increasing R concentrations. In the present investigations for Ba<sub>1-x</sub>La<sub>x</sub>F<sub>2+x</sub> we have not observed this complicated behavior, which has been associated by Meuldijk and den Hartog<sup>15</sup> with clustering of R<sup>3+</sup>-F<sub>i</sub><sup>-</sup> complexes. In Ba<sub>1-x</sub>La<sub>x</sub>F<sub>2+x</sub> the value of  $T_{\max}$  decreases gradually with increasing La concentrations. This behavior can be described perfectly well by a percolation-type charge-transport mechanism in which simple dipolar defects play an important role up to high concentrations (see also den Hartog and Langevoort<sup>27</sup>).

We assume that the HT band, which is ascribed to the relaxation of space charges, shifts to low temperatures because there is a gradual change of the charge-transport mechanism connected with this band. The relaxation time associated with the space-charge relaxation has been written as

$$\frac{1}{\tau} = \frac{\alpha}{\tau_{\text{dip}}} + \frac{1-\alpha}{\tau_{\text{free int}}}, \quad (6)$$

where  $\tau_{\text{dip}}$  and  $\tau_{\text{free int}}$  are the relaxation times of a jumping interstitial in the neighborhood of a trivalent La impurity or a free interstitial fluoride ion, respectively.  $\alpha$  is a parameter (see Refs. 27 and 17 for the precise definition) giving the relative probability for a dipole jump to occur in the charge-transport mechanism. It is clear that the value of  $\alpha$  increases with the concentration of La<sup>3+</sup>-F<sub>i</sub><sup>-</sup> dipoles. We have found that for concentrations larger than 2.2 mol % the relation between  $\alpha$  and  $x$  is

$$\alpha = A(x - 0.022)^{1.8}, \quad (7)$$

and for concentrations lower than 0.022,  $\alpha$  is very small. It should be noted that Eq. (7) is very similar to the usual relationship found for percolation conduction.<sup>28,29</sup> In an earlier paper we have argued that the threshold concentration of 2.2 mol % is approximately equal to a volume fraction of 25 vol %; i.e., a critical concentration, which is found in most percolating systems.

We have analyzed the results for  $T_{\max}$  of the HT peak and it has been found that the relaxation time as given in Eq. (6) can be used quite well to understand the observed behavior. The only assumption we must make is that there is no tendency toward clustering. The assumption has been justified for low concentrations by means of our extensive EPR investigations. For very high concentrations the EPR technique is not suitable anymore. Indirect information concerning the clustering processes have been obtained from the ITC results because we have observed that in some systems where extensive clustering has been observed with high-resolution spectroscopy,<sup>8-10</sup> the space-charge-relaxation band shows a complex behavior.

The only problem with the ITC data occurs for low La concentrations. In Fig. 9 we observe that in the concentration range  $10^{-4} \leq x \leq 10^{-2}$  the value of  $T_{\max}$  decreases continuously with increasing  $x$ . In comparable systems Sr<sub>1-x</sub>R<sub>x</sub>F<sub>2+x</sub> we have observed that for low R concentrations the value of  $T_{\max}$  is constant.<sup>14-17</sup> From our results on the system Ba<sub>1-x</sub>Na<sub>x</sub>F<sub>2+x</sub> we know that the charge transport by jumping vacancies in the anion sublattice is a slow process as compared with transport due to interstitial

fluoride ions. If in crystals of the type  $Ba_{1-x}La_xF_{2+x}$  monovalent cations or divalent anions (e.g.,  $O^{2-}$ ) are present there is a possibility that anion vacancies are dominant over the interstitial fluoride ions. In that case the space-charge-relaxation peak position is determined by the jump frequency of anion vacancies, whereas for crystals doped with sufficient amounts of  $La^{3+}$  this position is determined by the jump frequency of interstitial fluoride ions. From the shape of the curve representing the behavior of  $T_{max}$  vs  $\log_{10} x$  we estimate that the HT band associated with the jumps of free interstitial fluoride ions is located at  $T_{max} = 275\text{--}285$  K. It can be seen from Fig. 9 that according to our explanation in samples with

$x < 10^{-3}$  the vacancies contribute considerably to the space-charge relaxation.

#### ACKNOWLEDGMENTS

The authors wish to thank Mr. P. Wesseling for growing the crystals and providing technical assistance. This work is part of the research program of the Stichting Fundamenteel Onderzoek der Materie (Foundation for Fundamental Research on Matter—FOM) and has been made possible by financial support from the Nederlandse Organisatie voor Zuiver Wetenschappelijk Onderzoek (Netherlands Organization for the Advancement of Pure Research—ZWO).

- 
- <sup>1</sup>E. L. Kitts, Jr., M. Ikeya, and J. H. Crawford, Jr., *Phys. Rev. B* **8**, 5840 (1977).  
<sup>2</sup>A. D. Franklin and S. Marzullo, *J. Phys. C* **3**, L171 (1970).  
<sup>3</sup>A. Edgar and H. K. Welsh, *J. Phys. C* **12**, 703 (1979).  
<sup>4</sup>P. W. M. Jacobs and S. H. Ong, *J. Phys. Chem. Solids* **41**, 431 (1980).  
<sup>5</sup>B. P. M. Lenting, J. A. J. Numan, E. J. Bijvank, and H. W. den Hartog, *Phys. Rev. B* **14**, 1811 (1976).  
<sup>6</sup>W. van Weperen and H. W. den Hartog, *Phys. Rev. B* **18**, 2857 (1978).  
<sup>7</sup>A. B. Aalbers and H. W. den Hartog, *Phys. Rev. B* **19**, 2163 (1979).  
<sup>8</sup>D. R. Tallant and J. C. Wright, *J. Chem. Phys.* **63**, 2074 (1975).  
<sup>9</sup>D. R. Tallant, D. S. Moore, and J. C. Wright, *J. Chem. Phys.* **67**, 2897 (1977).  
<sup>10</sup>D. S. Moore and J. C. Wright, *Chem. Phys. Lett.* **66**, 173 (1979).  
<sup>11</sup>D. S. Moore and J. C. Wright, *J. Chem. Phys.* **74**, 1626 (1981).  
<sup>12</sup>J. Corish, C. R. A. Catlow, P. W. M. Jacobs, and S. H. Ong, *Phys. Rev. B* **25**, 6425 (1982).  
<sup>13</sup>M. C. Wintersgill, J. J. Fontanella, P. Welcher, R. J. Kimble, and C. G. Andeen, *J. Phys. C* **13**, L661 (1980).  
<sup>14</sup>J. Meuldijk, G. Kiers, and H. W. den Hartog, preceding paper, *Phys. Rev. B* **28**, 6022 (1983).  
<sup>15</sup>J. Meuldijk and H. W. den Hartog, *Phys. Rev. B* **27**, 6376 (1983).  
<sup>16</sup>J. Meuldijk and H. W. den Hartog, *Phys. Rev. B* **28**, 1036 (1983).  
<sup>17</sup>J. Meuldijk, H. H. Mulder, and H. W. den Hartog, *Phys. Rev. B* **25**, 5204 (1982).  
<sup>18</sup>E. J. Bijvank, H. W. den Hartog, and J. Andriessen, *Phys. Rev. B* **16**, 1008 (1977).  
<sup>19</sup>E. J. Bijvank and H. W. den Hartog, *Phys. Rev. B* **22**, 4133 (1980).  
<sup>20</sup>E. Laredo, M. Puma, N. Suarez, and D. R. Figueroa, *Phys. Rev. B* **23**, 3009 (1981).  
<sup>21</sup>A. N. Lefferts, E. J. Bijvank, and H. W. den Hartog, *Phys. Rev. B* **17**, 4214 (1978).  
<sup>22</sup>W. van Weperen, B. P. M. Lenting, E. J. Bijvank, and H. W. den Hartog, *Phys. Rev. B* **16**, 2164 (1977).  
<sup>23</sup>L. A. Boatner, R. W. Reynolds, and M. M. Abraham, *J. Chem. Phys.* **52**, 1248 (1970).  
<sup>24</sup>A. K. Cheetham, B. E. F. Fender, and M. J. Cooper, *J. Phys. C* **4**, 3107 (1971).  
<sup>25</sup>C. R. A. Catlow, *J. Phys. C* **9**, 1845 (1976).  
<sup>26</sup>H. W. den Hartog, *Phys. Rev. B* **27**, 20 (1983).  
<sup>27</sup>H. W. den Hartog and J. C. Langevoort, *Phys. Rev. B* **24**, 3547 (1981).  
<sup>28</sup>S. Kirkpatrick, *Rev. Mod. Phys.* **45**, 574 (1973).  
<sup>29</sup>P. A. Lightsey, Ph.D. thesis, Cornell University, 1972 (unpublished).